Materials Science-Poland, Vol. 27, No. 2, 2009

Hydrothermal synthesis and characterization of tube-structured ZnO needles

Y. LI*, H. FENG, N. ZHANG, C. LIU

College of Science, Civil Aviation University of China, Tianjin, 300300, P.R. China

Tube-structured ZnO needles were successfully synthesized hydrothermally, using H_2O_2 as the solvent, Zn $(NO_3)_2 \cdot 6H_2O$ and NaOH as the starting materials and $C_{19}H_{42}BrN$ as the additive. The samples were characterized by scanning electron microscopy, X-ray diffraction and room temperature photoluminescence measurements. The as-synthesized ZnO needle possesses a tube structure coiled by multilayer along the [0001] direction and a wurtzite structure. The intensity of the (0002) diffraction peak is obviously lower than the $(10\bar{1}0)$ and $(10\bar{1}1)$ peaks. Photoluminescence results reveal that the UV emission is restrained as hydrothermal temperature increases, and that the concentration of H_2O_2 has no influence on the photoluminesence when the concentration of H_2O_2 is higher than 10%.

Key words: *zinc oxide; hydrothermal synthesis; photoluminescence; morphology; tube*

1. Introduction

Zinc oxide (ZnO) is one of the important prospective short wavelength emitters owing to its large excitation binding energy and a wide energy gap of 3.3 eV at room temperature. It is also a material suitable for generating ultraviolet (UV) light [1]. Furthermore, high exciton binding energy of about 60 meV in ZnO, which is significantly larger than the thermal energy at room temperature (26 meV), can ensure an efficient exciton emission at room temperature [2, 3]. Owing to these properties, zinc oxide is widely used in various applications such as photonic devices [4], solar cell windows [5], plasma display panels [6], surface acoustic wave devices [7], and gas sensors [8]. It is well-known that the optical, electrical and magnetic properties of zinc oxide are markedly influenced by its microstructure and morphology [9]. Therefore, various morphological crystallites of zinc oxide, such as nanorods [10], and microflowers

*Corresponding author, e-mail address: liyan01898@163.com

[11], nanorings [12], nanowires [13] have been synthesized via different methods. Needle-shaped nano zinc oxide has been synthesized by the wet chemical method [14] and solid-vapour method [15]. In this paper, a novel tube-structured ZnO needles were successfully synthesized hydrothermally. The morphologies and photoluminescence of ZnO needles were characterized by XRD, SEM and PL methods. A multilayer structure, namely a spiral growth line and a honeycomb structure, not reported in the above references, have been found in our experiment.

2. Experimental

Nitrate hexahydrate ($Zn(NO_3)_2 \cdot 6H_2O$), sodium hydroxyl (NaOH), hydrogen peroxide (H_2O_2, 30%) and N,N,N-trimethyl-1-hexadecanaminium bromide (CTABr, $C_{19}H_{42}BrN$) were analytical grade reagents, purchased commercially and used without further purification.

The ZnO needles were prepared according to the following process. 0.1 M aqueous solution of $Zn(NO_3)_2 \cdot 6H_2O$ and 0.2 M solution of NaOH were all prepared with deionized water. NaOH solution was added to zinc nitrate solution drop by drop at room temperature under vigorous stirring which resulted in formation of a white suspension. The suspension was then separated with a centrifuge and washed three times with distilled water, and then finally washed with absolute alcohol. The separated powder was dried at 70 °C for 24 h in an oven to obtain the precursor. Subsequently, 2 g of precursor materials and CTABr were added to 30 cm^3 of H_2O_2 solution and the mixture was stirred and then sealed into a Teflon-lined autoclave with a filling capacity of about 35%. The autoclave was treated by hydrothermal method. Two batches of ZnO samples were obtained under different conditions. The first batch was synthesized at 70 °C, 90 °C, 120 °C, 150 °C and 180 °C for 12 h in a mixture of 30 cm^2 H_2O_2 (30%) and 0.1 g CTABr. The other batch was synthesized at 120 °C for 12 h in 30%, 25% and 10% H_2O_2 solutions. The resulting white precipitates were collected and washed with distilled water and alcohol for several times to obtain ZnO crystallites.

The morphology of ZnO particles was observed with a 1530VP model field emission scanning electron microscope (SEM) and Axioskop 40 Pol optical microscope. X-ray diffraction (XRD) with CuK_α radiation (λ = 0.1542 nm) on DX-2000 X-ray diffractometer was used for checking the formation and identification of compounds present in the obtained particles. Photoluminescence (PL) spectra of ZnO nanocrystals were recorded with a WGY-10 fluorescence spectrophotometer equipped with a Xe lamp (150 mW). The excitation wavelength was 325 nm. The emission spectrum of solid zinc oxide powder samples at room temperature was observed in the wavelength range of 350–650 nm.

3. Results and discussion

3.1. Powder X-ray diffraction analysis

Figure 1 shows the X-ray diffraction (XRD) patterns of as-obtained ZnO crystallites synthesized hydrothermally at various temperatures. In Figure 1, curves c–e, the the ZnO crystals possess a wurtzite structure and the diffraction peaks can be well indexed to hexagonal ZnO with the lattice parameters a = 0.324982 nm and c = 0.520661 nm. Although the peaks of $(10\bar{1}0)$ and $(10\bar{1}1)$ planes in Fig. 1, curves a, b are uniform

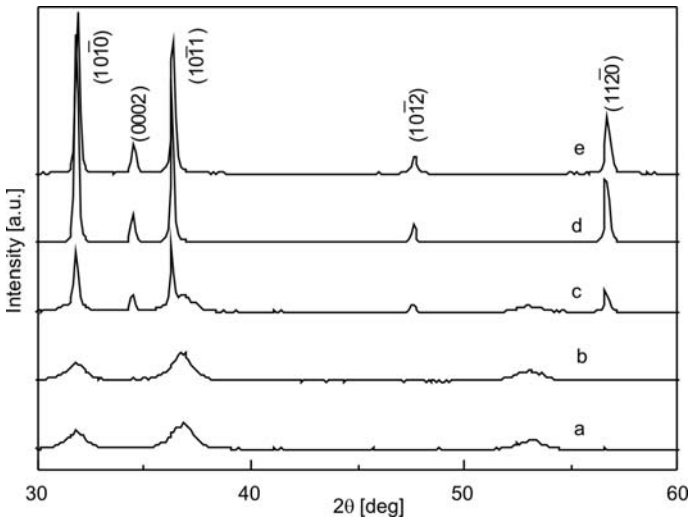

Fig. 1. XRD patterns of ZnO needles synthesized at: a) 70 °C, b) 90 °C, c) 120 °C, d) 150°C, e) 180°C

with that in Fig. 1c–1e (0002), $(10\bar{1}2)$ and $(11\bar{2}0)$ peaks are not visible due to small sizes and lower dimension of the samples synthesized at lower temperature. Meanwhile, the intensity of the (0002) peak in Fig. 1 is obviously lower those of the peaks $(10\bar{1}0)$ and $(10\bar{1}1)$. This result seems to be in conflict with the long needle shaped morphology (Fig. 2) grown quickly along the [0001] direction. In fact, the low intensity of the (0002) peak is caused by a small area of (0001) cross section and a thin multilayer wall of the tube-structured needle. Upon increasing hydrothermal temperature, the diffraction peaks intensities of five polar planes increase substantially, because the growth rate of ZnO increases when the temperature is raised.

3.2. Morphology of ZnO samples

Figure 2 shows the morphology of the synthesized ZnO. Samples synthesized at various temperatures have similar morphologies to that in Fig. 2 besides having larger dimensions at higher temperatures.

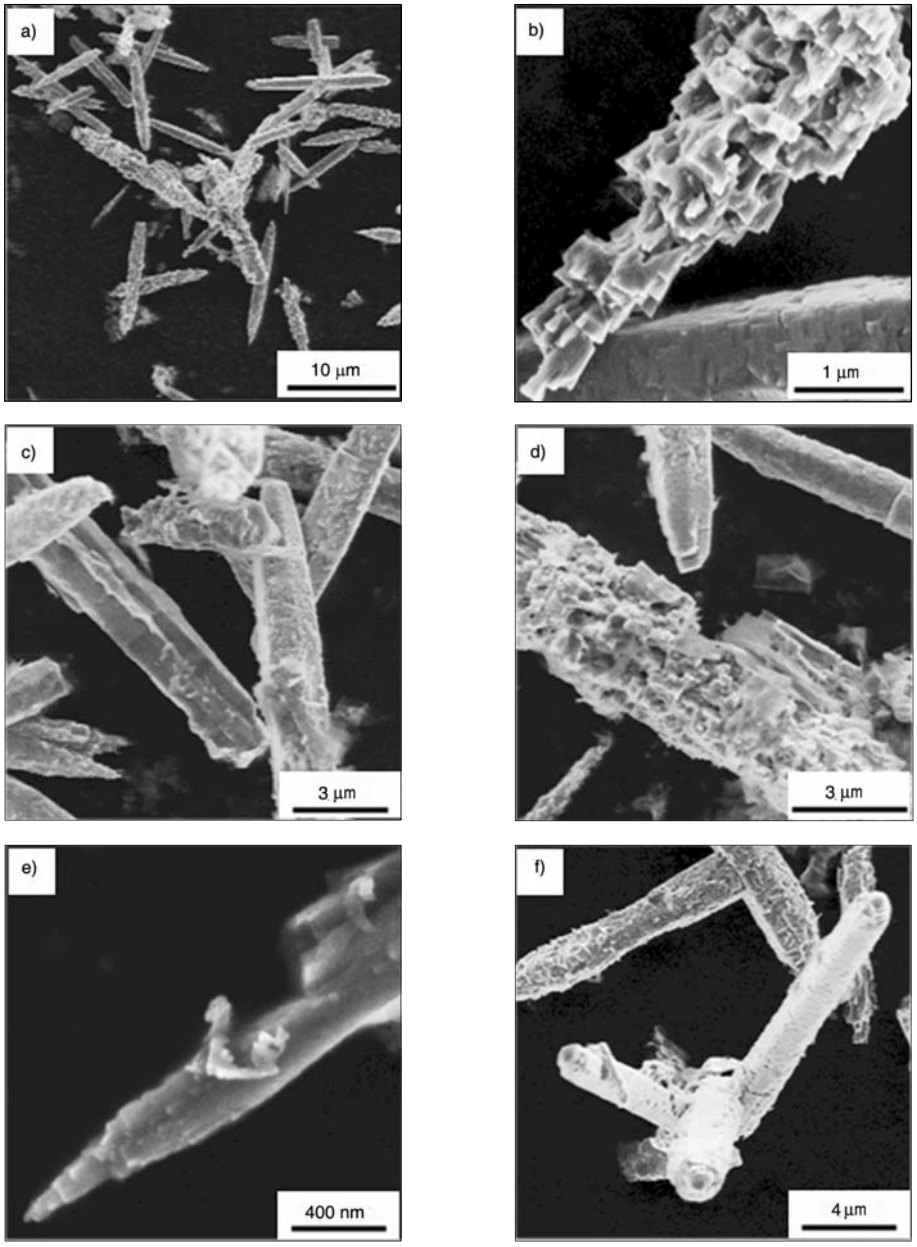

Fig. 2. SEM images of tube-structured ZnO needles synthesized at 180 °C for 48 h

The tube-structured ZnO needles in Fig. 2, with a thin (up to 50 nm) and long (up to 1 μm) tips (Figs. 2a, e), are 5–10 μm long, 500–1000 nm in external diameter and 100–200 nm (Fig. 2f) in inner diameter. The local wall thickness of the tube is ca.

100–150 nm. A random honeycomb structure, decorticated needles resulting from experimental processing, coiled by belts or layers with the width of about 200 nm and 50–100 nm thick are observed in Fig. 2b, d, and the remains of the surface layers can be seen in Fig. 2d. The top (0001) and bottom $(000\bar{1})$ surfaces are partly or completely opened (Fig. 2f) and some cracks and holes are observed in the side surface wall as shown in Figs. 2c, f. Interestingly, for some needles, the inner layer and outer layer and the interstice between the layers can be clearly observed (cf. Fig. 2c). Furthermore, some tubes derived from layer coiling along the [0001] direction with a multilayer wall were found, the hatch and some cracks could be seen in the tube end in the middle of Fig. 2f. The spiral lines formed by the layer coiling approach during the growth of ZnO needles could be clearly observed in Fig.2e. It is reasonable to suggest that these needle-shaped ZnO tubes with polycrystalline walls consist of wurtzite-type ZnO layers. It is implied that the supersaturation near the side surface of the growing crystal is higher than that at the centre, leading to preferential stronger nucleation and growth along the [0001] direction of the side surface. Furthermore, hydrogen peroxide could support the growth along the [0001] direction and the side-face by providing enough oxygen. The most likely growth mechanism is that described in the references [16]: an initially grown sheet turns into a roll and the cone-shaped roll transforms into a cylindrical tube, presumably via a dislocation “zipper” mechanism. Finally, a hollow tube transforms into a needle.

3.3. Photoluminescence

Figure 3 presents the photoluminescence (PL) spectra of the as-prepared ZnO crystallites fabricated at various temperatures, excited with 325 nm UV light from a He-Cd laser at room temperature. A typical emission spectrum consists of a peak at ca. 400 nm, a broad blue emission at ca. 410–470 nm, and a narrow green one at ca. 550 nm. The visible emission is usually considered to be related to various intrinsic defects produced during preparation of ZnO and post-treatment. Normally, these defects are located at the surface of the ZnO structure. The blue emission corresponds to the zinc vacancy and oxygen vacancy; the zinc vacancy forms a shallow acceptor level and the oxygen vacancy forma a shallow donor level [17]. There are two kinds of transitions for blue emission: one is electron transition from conduction band to the shallow acceptor level formed by zinc vacancy, the other is an electron transition from the shallow donor level formed by oxygen vacancy to the valence band. The UV emission corresponds to the near band-edge emission resulting from the recombination of free excitons.

Figure 3 shows that the UV emission gradually diminishes, while the blue emission intensity increases and the UV peaks cannot be observed in Fig. 3, curves d and e. It implies that the blue emission probability is higher than that of the UV emission due to the concentration of zinc vacancies and oxygen vacancies increasing as the hydro-

thermal temperature increases. The green emission is commonly referred to as the singly ionized oxygen vacancy and the emission results from the radiative recombination of photo generated holes with electrons occupying oxygen vacancies [18].

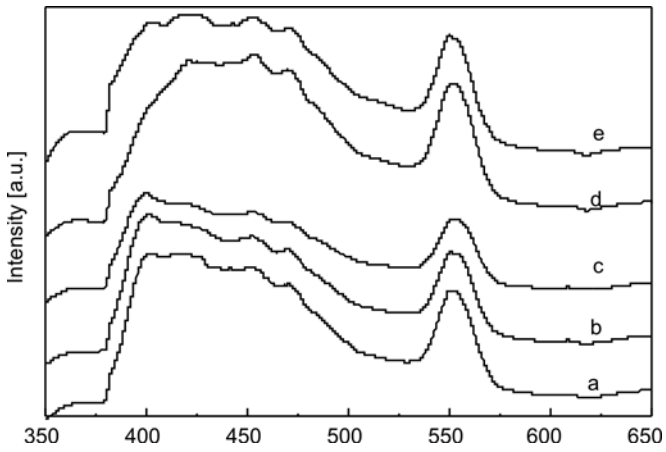

Fig. 3. Room temperature photoluminescence spectrum of ZnO needles hydrothermally synthesized at: a) 70 °C, b) 90 °C, c) 120 °C, d) 150 °C, e) 180 °C

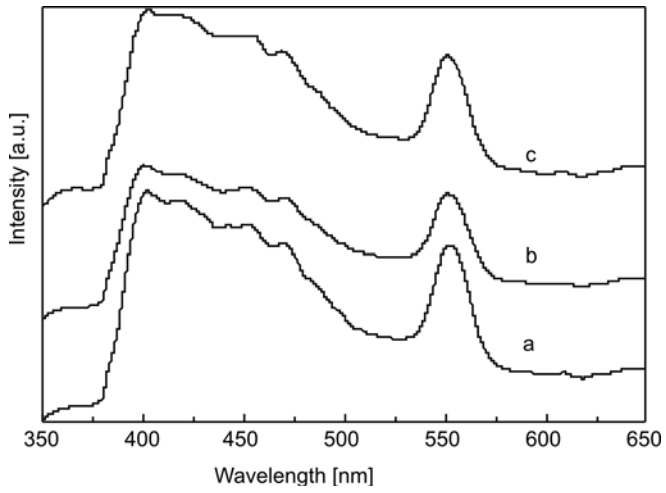

Fig. 4. Room temperature photoluminescence spectrum of ZnO needles synthesized in: a) 30%, b) 25%, c) 10% H_2O_2 solution

The room temperature PL spectra of the ZnO nanoneedles (batch 2) fabricated for three different quantities of H_2O_2 were recorded as shown in Fig. 4. A broad UV-blue emission peak scatters at around 400 to 470 nm and a green emission peak centred at about 550 nm are observed in Fig. 4. It is found that concentration of H_2O_2 has no influence on the PL properties when the concentration of H_2O_2 is higher than 10%.

4. Conclusion

Tube-structured ZnO needles were successfully synthesized via a hydrothermal method in H_2O_2 solution. It was found that ZnO needles possess a tube structure encircled by multilayer along the *c*-axis. Hydrogen peroxide could support the growth along *c*-axis and the side-face by providing enough oxygen. The XRD spectroscopy results show that each ZnO needle has a wurtzite structure, and the weak intensity of the (0002) peak is caused by the small area of (0001) cross section and a thin multilayer wall of the tube-structured needle. PL results reveal that the blue emission probability is greater than that of the UV emission as increasing the hydrothermal temperature or the concentration of H_2O_2 has no influence on the PL properties when the concentration of H_2O_2 is higher than 10%.

Acknowledgements

We thank the Tianjin Natural Science Foundation (05yfJMTC 12900) for financial support.

References

[1] KIM D.K., MANOR U., Scripta Mater., 54 (2006), 807.
[2] CHEN Z., GAO Q.M., ROAN M., SHI J.L., Appl. Phys. Lett., 87 (2005), 93113.
[3] VOROB'EV V.A., J. Opt. Techn., 72 (2005), 47.
[4] YATSUI T., SANGU S., KAWAZOE T., OHTSU M., AN S.J., YOO J., YI G.C., Appl. Phys. Lett., 90 (2007), 223110.
[5] BHOSLE V., PRATER J.T., YANG F., BURK D., FORREST S.R., NARAYAN J., J. Appl. Phys., 102 (2007), 023501.
[6] YOON S.H., YANG H., KIM Y.S., J. Ceram. Process. Res., 8 (2007), 261.
[7] SHIH W.C., WANG M.J., LIN I.N., Diamond Relat. Mater., 17 (2008), 390.
[8] LIAO L., LU H.B., SHUI M., LI Y.L., LIU C., SHEN Z.X., YU T., Nanotechn., 19 (2008), 175501.
[9] ANDELMAN T., GONG Y.Y., POLKING M., KUSKOVSKY I., NEUMARK G., O'BRIEN S., J. Phys. Chem., 109 (2005), 14314.
[10] TEKI R., PARKER T.C., LI H.F., KORATKAR N., LU T.M., LEE S., Thin Solid Films., 516 (2008), 4993.
[11] LIU J.P., HUANG X.T., LI Y.Y., DUAN J.X., AI H.H., REN L., Mater. Sci. Eng. B., 127 (2006), 85.
[12] PENG Y., BAO L., Chem. J. Chin. Univ., 29 (2008), 28.
[13] WANG Z.L., J. Nanosci. Nanotechnol., 8 (2008), 27.
[14] YADAV R.S., PANDEY A.C., Physica E., 40 (2008), 660.
[15] FAN H.J., LOTNYK A., SCHOLZ R., YANG Y., KIM D.S., PIPPEL E., SENZ S., HESSE D., ZACHARIAS M., J. Phys. Chem., 112 (2008), 6770.
[16] POKROPIVNY V.V., KASUMOV M.M., Techn. Phys. Lett., 33 (2007), 44.
[17] WANG Q.P., ZHANG X.J., WANG G.Q., CHEN S.H., WU X.H., MA H.L., Appl. Surf. Sci., 254 (2008), 5100.
[18] DAI Y., ZHANG Y., BAI Y.Q., WANG Z.L., Chem. Phys. Lett., 375 (2003), 96.

Received 24 June 2008
Revised 22 December 2008